Jet stream intraseasonal oscillations drive dominant ecosystem variations in Oregon's summertime coastal upwelling system

John M. Bane*[†], Yvette H. Spitz[‡], Ricardo M. Letelier[‡], and William T. Peterson[§]

*Department of Marine Sciences, University of North Carolina, Chapel Hill, NC 27599-3300; [‡]College of Oceanic and Atmospheric Sciences, Oregon State University, Corvallis, OR 97331-5503; and [§]National Oceanic and Atmospheric Administration/National Marine Fisheries Service, Newport, OR 97365

Edited by Jane Lubchenco, Oregon State University, Corvallis, OR, and approved June 26, 2007 (received for review February 1, 2007)

Summertime wind stress along the coast of the northwestern United States typically exhibits intraseasonal oscillations (ISOs) with periods from ≈15 to 40 days, as well as fluctuations on the 2- to 6-day "weather-band" and 1-day diurnal time scales. Coastal upwelling of cool, nutrient-rich water is driven by extended periods of equatorward alongshore winds, and we show that the ≈20-day ISOs in alongshore wind stress dominated the upwelling process during summer 2001 off Oregon. These wind stress ISOs resulted from north–south positional ISOs of the atmospheric jet stream (JS). Upper-ocean temperature, phytoplankton, and zooplankton varied principally on the ≈20-day time scale as well, and these correlated with the ISOs in alongshore wind stress and JS position, even though there also were weather-band stress fluctuations of comparable magnitude. Such wind stress ISOs are typical along Oregon in the summer upwelling season, occurring in 10 of 12 years examined, including 2001. We present a previously unreported direct connection from the atmospheric JS to oceanic primary and secondary production on the intraseasonal time scale and show the leading importance of ISOs in driving this coastal upwelling ecosystem during a typical summer.

coastal variability | wind-driven ocean upwelling | coastal marine ecosystems | marine ecology

Intraseasonal oscillations (ISOs) are fluctuations in the atmosphere–ocean system with periods between 10 and 100 days (1). Wind stress is known to fluctuate with intraseasonal periodicities, and wind stress ISOs can affect coastal marine environments in important ways (2–4). This became strikingly apparent during the summer 2001 Coastal Ocean Advances in Shelf Transport (COAST) observational program in the central Oregon upwelling system. The observed May–August alongshore wind stress was composed of 20-day ISOs, 2- to 6-day "weather-band" fluctuations [mostly due to the passage of synoptic scale atmospheric extratropical cyclones (ETCs)], and smaller diurnal variations. The 20-day ISOs were driven by similar-period oscillations in the north-south position of the atmospheric jet stream (JS). Such midlatitude, JS-driven atmospheric ISOs have only recently been recognized (5, 6), and we show here that they can have important, even dominant impacts on the coastal ocean.

Data from other years show that summertime wind stress ISOs of similar periods and character are typical off Oregon, although during 2 summers of the 12 examined they did not appear (3). This indicates that 2001 was a typical year in terms of intraseasonal wind stress variability in this region, and the coastal responses that were observed then are described herein. In a related paper (4), anomalous conditions that occurred in this region during summer 2005 are described. Those conditions occurred when the JS over the NE Pacific was positioned more southward than normal through early July, significantly delaying the beginning of the 2005 upwelling season off Oregon. The ISO activity then drove downwelling winds. The more typical 2001 conditions described here can be contrasted with the anomalous ecosystem conditions during 2005, as well as with conditions from other years as new analyses become available.

The dominant fluctuations in upper-ocean temperature and chlorophyll observed off central Oregon during 2001 occurred on the 20-day time scale, with minor contributions at other periodicities. Significant correlations between these property ISOs and the wind stress ISOs at time lags of a few days (Table 1) support the conclusion that wind stress ISOs drove them through the modulation of coastal upwelling (3, 7, 8). Observed and modeled time series indicate that the 20-day oscillations in phytoplankton set the dominant time scale for zooplankton as well (7). Here we present observations and model simulations to demonstrate the importance of ISOs in this coastal system during a typical upwelling season. We demonstrate a previously unreported connection from the atmospheric JS to oceanic primary and secondary production variations on the intraseasonal time scale and show the leading importance of ISOs in this coastal upwelling ecosystem during typical summers.

Atmospheric Circulation and ISOs in the Northeast Pacific

Three major atmospheric pressure systems give rise to the surface winds over the northeast Pacific in summer (Fig. 1 *Lower*). These are the maritime North Pacific High, the continental Thermal Low, and the Aleutian Low. The last is an area of average low pressure over Alaska that is primarily the result of a number of ETCs (often called "Gulf of Alaska Lows" in this region) that traverse eastward through the area. A several-day-long episode of southward winds off Oregon typically results when a JS positional ISO is in a northern phase (Fig. 1 *Left Upper*). This is because the northward movement of the JS for half of the ≈20-day ISO period allows the North Pacific High to "build in" and dominate along the U.S. west coast (Figs. 1 *Left Lower* and 2*d*).

Interruptions of these periods of persistent southward winds by northward-wind events typically happen when the JS moves to the south, usually ≈500–1,000 km from its northward ISO position (Fig. 1 *Right Upper*). This shifts the tracks of ETCs southward far enough that they will impinge on the northwestern U.S. coast, causing periods of pre-cold-frontal northward winds that typically last a day or so (Figs. 1 *Right Lower* and 2*d*). Additionally, northward-propagating coastally trapped wind reversals will occasionally bring northward winds (9, 10).

JS ISOs have been examined (5), and a relationship has been found between the Rocky Mountains' torque effect on the JS and the dominant patterns of intraseasonal variability in the surface pressure patterns over the North Pacific. A pressure

Author contributions: J.M.B., Y.H.S., R.M.L., and W.T.P. designed research; J.M.B., Y.H.S., R.M.L., and W.T.P. performed research; J.M.B., Y.H.S., R.M.L., and W.T.P. analyzed data; and J.M.B., Y.H.S., R.M.L., and W.T.P. wrote the paper.

The authors declare no conflict of interest.

This article is a PNAS Direct Submission.

Abbreviations: ISO, intraseasonal oscillation; ETC, extratropical cyclone; JS, jet stream; COAST, Coastal Ocean Advances in Shelf Transport; MABL, marine atmospheric boundary layer; NDBC, National Data Buoy Center; 8-DLP, 8-day low-passed; 36-HLP, 36-hr low-pass.

[†]To whom correspondence should be addressed. E-mail: bane@unc.edu.

 www.pnas.org/cgi/doi/10.1073/pnas.0700926104

Table 1. Correlations and temporal lags between time series

Time series pair	Correlation coefficient	Significance level, %	Lag, days
JS position (inverted) and stress	0.60	95	0.0
Stress and ocean temperature	0.56	95	3.2
Stress and model phytoplankton	−0.47	90	7.4
Stress and observed Chl-a	−0.58	95	13.6
Stress and model zooplankton	−0.40	90	13.2

Each time series has been 8- to 35-day band-passed to determine the correlations between ISOs in that period band, which contains the dominant intraseasonal variance. In each case the second time series follows the first by the specified time lag. The significance of each correlation is greater than the level shown. Stress and ocean temperature refer to alongshore wind stress and upper-ocean temperature, respectively, at NDBC 46050. (see Fig. 4).

empirical orthogonal function (EOF) mode (at the 700-hPa level) was found to correlate best with the mountain torque in this period band, and it contains a "bull's-eye" pattern that is ≈3,000 km in diameter and centered near 45°N 140°W, with significant spectral energy between 20 and 30 days. This alternating high/low pressure anomaly is situated such that it

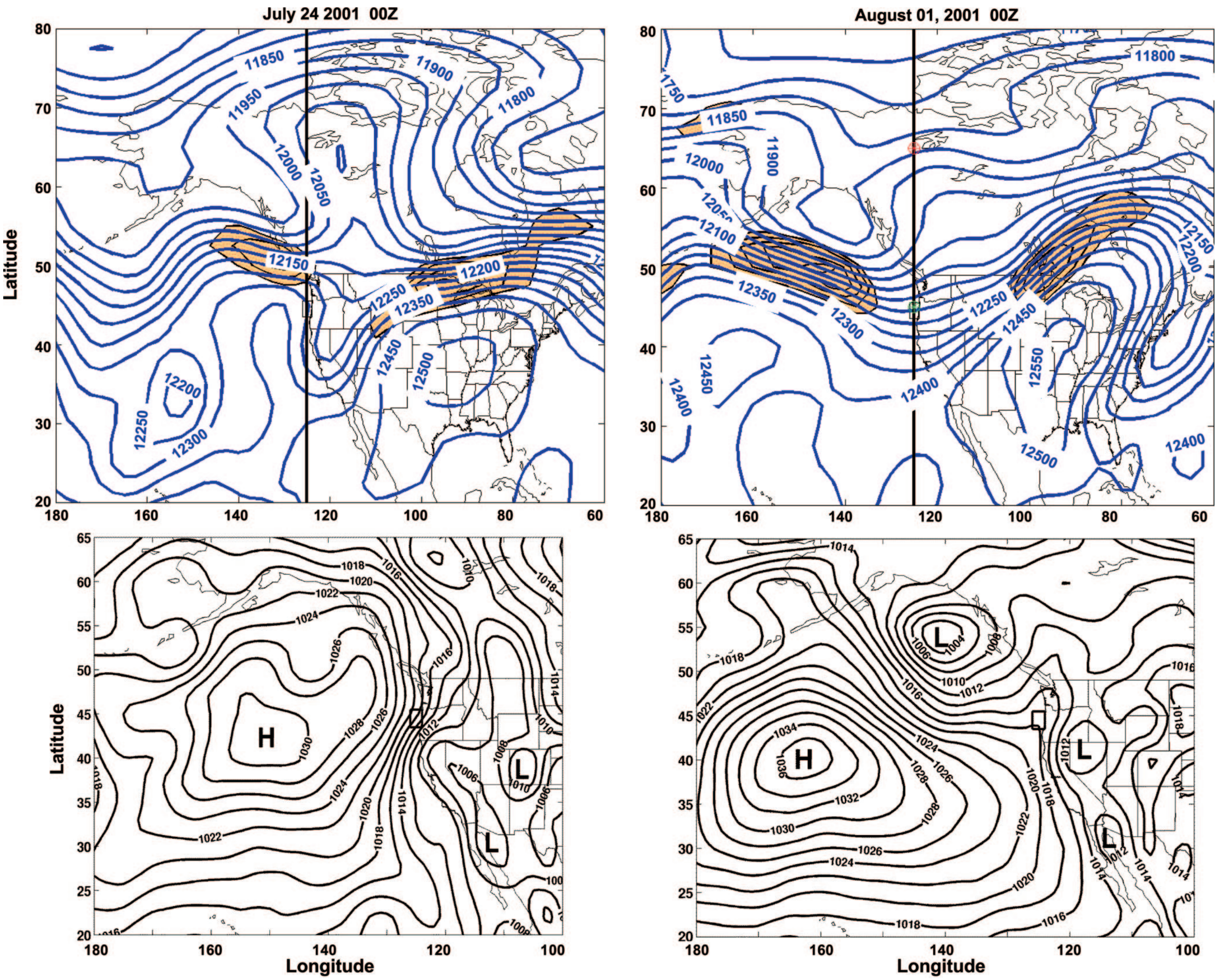

Fig. 1. Atmospheric conditions during a typical JS ISO (northward phase, *Left*; southward phase, *Right*). JS flow (as indicated by the height of the 200 hPa pressure surface; *Upper*) and surface atmospheric pressure patterns (*Lower*) on July 24, 2001 (*Left*) and August 1, 2001 (*Right*). H indicates the center of the North Pacific High pressure system, and L indicates either the Thermal Low (*Left* and *Right*, over land) or an eastward traveling ETC (*Right*, over water south of Alaska). Conditions on these days were typical of: (*Left*) southward, upwelling-favorable winds in the COAST area (rectangle off Oregon coast) associated with the dominance of the North Pacific High throughout the region when the JS is in a northward ISO phase, and (*Right*) northward, downwelling-favorable winds at COAST driven by a passing Gulf of Alaska Low (the ETC centered at ≈54N 140W) when the JS ISO is in a southward phase. In the upper panels, the vertical line denotes 125 West longitude, through the COAST study region, and the shading represents the regions of greatest wind speed in the JS.

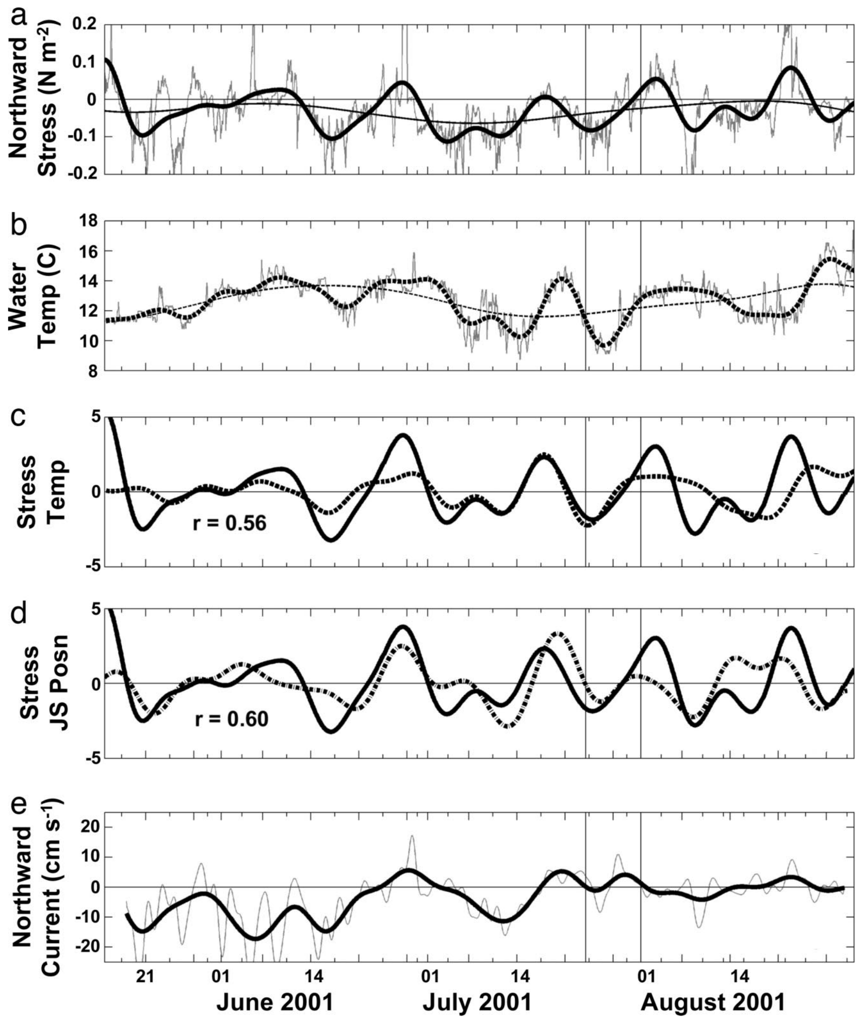

Fig. 2. Time series of several physical variables in the COAST domain for the period of the summer 2001 field experiment. (*a*) Northward wind stress at NDBC buoy 46050 (thin line is measured, thick line is 8-DLP, medium line is 35-DLP). (*b*) Upper-ocean temperature from the same buoy (thin line, measured; thick dashed line, 8-DLP; thin dashed line, 35-DLP). (*c*) The 8- to 35-DBP stress and temperature time series shown together, with a 3-day lead applied to temperature and stress scaled to fit the vertical axis (note the sequence of 20-day temperature ISOs and the high coherence these have with the stress ISOs; correlation $r = 0.56$, significant at the 95% level). (*d*) Wind-stress time series together with the JS location time series (both curves are 8- to 35-DBP; vertical axis is degrees of latitude for JS position, same scale for stress as used in *c*; the JS position curve has been inverted so that a southward position is toward the top of the image; note the strong coherence between the stress and JS position time series; correlation $r = 0.60$, significant at the 95% level). (*e*) Alongshore velocity measured at 10 m below the ocean surface at a COAST mooring on the 100-m isobath $\approx$35 km south of 46050. The two vertical lines denote the days shown in Fig. 1.

drives intraseasonal wind variations along Oregon, consistent with the COAST observations.

Meteorology During COAST-2001

Using data from National Data Buoy Center (NDBC) buoy 46050 (35 km offshore of Newport, OR; see Fig. 4), Fig. 2*a* shows that 20-day ISOs were the dominant form of wind-stress variability with periods between 2 and 100 days during COAST [compare the 8-day low-passed (8-DLP) and unfiltered curves]. These ISOs and the 2- to 6-day weather-band oscillations had approximately equal stress amplitudes of ≈ 0.1 N m^{-2}; however, the ISOs occurred for essentially the entire experiment period, whereas the weather-band fluctuations were intermittent, being weak or absent for up to a week or so at times (Fig. 3*a*). The correlation between wind-stress ISOs and those in the north–south position of the JS is apparent in Fig. 2*d*, with a maximum correlation of $r = 0.60$ (significant at 95%) at zero lag. Note that this correlation was determined for the alongshore wind stress and the inverted JS position, because it is the northward (or positive) movement of the JS that causes the southward (or negative) wind stress during an ISO. Table 1 shows correlations between several additional time series pairs.

The marine atmospheric boundary layer (MABL) along the U.S. west coast during summer usually comprises a cool, well mixed layer immediately above the ocean surface (usually several hundred meters to >1 km thick) and a capping inversion layer above, in which the *in situ* temperature increases with height. There is often a slope to the inversion layer, which gives a baroclinic effect that produces a low-level wind jet within the MABL just above the ocean surface. This baroclinicity is relatively small off Oregon but can become substantial farther to the south. During northward wind episodes brought on by ETCs, the MABL temperature stratification virtually disappears (3). The MABL is affected directly by the JS, in that the changes from southward winds (stratified and sometimes baroclinic MABL) to northward winds (little MABL stratification) are largely dictated by the JS position, on both the weather-band and intraseasonal time scales. When southward winds are present, there can be a wind-stress curl effect brought about by the frictional drag of the coastal orography and the establishment of an internal boundary layer within the MABL

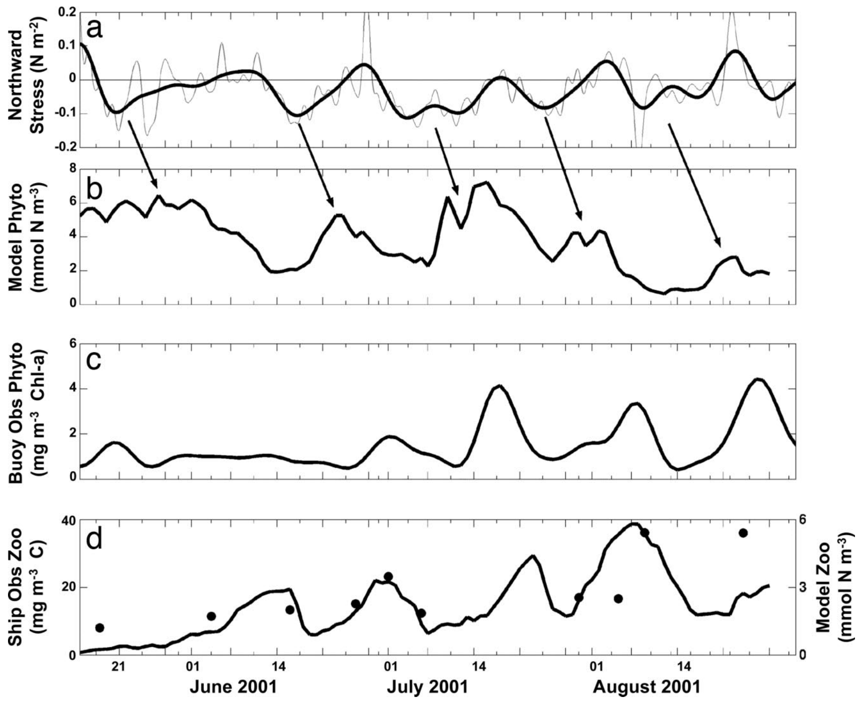

Fig. 3. Time series of several variables in the COAST domain for the period of the summer 2001 field experiment. Each variable shows clearly the series of five 20-day ISOs that occurred then. Both observed and modeled values are shown as follows. (*a*) Alongshore wind stress observed at NDBC 46050 [heavy curve, 8-DLP; light curve, 36-HLP wind stress, which was used to force the circulation/ecosystem model (7)]. (*b*) Unfiltered phytoplankton biomass from the ecosystem model [this is the average concentration for the Newport Line, spatially averaged from the surface to 60-m depth (or the bottom) and from the shoreline to the 200 m isobath]. (*c*) The 8-DLP observed phytoplankton biomass from the GLOBEC mooring located near the 200-m isobath on the Newport Line. (*d*) The curve is unfiltered zooplankton biomass from the ecosystem model (7) [this is the average concentration for the Newport Line (averaged in the same manner as phytoplankton)], and the filled dots show total copepod biomass measured at three locations on the Newport Line. The arrows indicate the phytoplankton maxima that followed the five southward stress ISOs by several days. Note that direct comparisons between observed and modeled plankton data will show quantitative differences due to the fixed-point sensor used in the field sampling vs. the section-averaged model values. The important feature to see is the appearance of 20-day ISOs in every variable.

over the cold upwelled water, which reduces wind speed there and produces a positive stress curl. The effect of this wind-stress curl on upwelling rate in the COAST region has been estimated to be ≈10–20% of effect due to Ekman transport divergence at the coastline (3). This stress curl will vary directly as the southward winds vary, which means the JS-driven ISO activity in stress will be reflected in the stress curl.

Physical Oceanography During COAST-2001

A sequence of ISOs in upper-ocean temperature, with peak-to-peak amplitudes up to 4°C, was observed throughout the COAST moored instrument array (Fig. 2*b*). At least five such oscillations occurred at each of the six COAST moorings (Fig. 4) and at NDBC 46050, and they occupied the entire COAST period. The upper-ocean temperature ISOs were the dominant temperature oscillation at each mooring location, with smaller variations at other periods. In contrast, the unfiltered wind stress (Fig. 2*a*, thin line) and alongshore velocity (Fig. 2*e*, thin line) time series have weather-band fluctuations that rival the ISOs in amplitude [see also the 36-hr low-pass (36-HLP) stress in Fig. 3*a*]. The correlation between the 8- to 35-DLP wind stress and upper-ocean temperature is a maximum when the stress time series is lagged by ≈3 days (Fig. 2*c*). The maximum correlation is $r = 0.56$ (significant at the 95% level) at a lag of 3.2 days (Table 1).

These time series are the signatures of the upwelling system's physical response on the two important time scales of 2- to 6-days (weather-band) and ≈20-days (ISOs). The alongshore oceanic flow responds at both periodicities approximately equally, but the ocean temperature does not, changing much more due to the ISO stress variations. The currents respond to the wind rather quickly (11, 12) and so will follow both the weather-band and intraseasonal forcing. Temperature decreases as upwelling progresses and the cold water covers more of the continental shelf, due either to the temperature front moving offshore (8) or to the cold water in the separated coastal upwelling jet moving downcoast (13). Taking advection as the principal cause of upper-ocean temperature decrease at a given location, the local rate of change of temperature will be proportional to the velocity, with the temperature gradient being the proportionality factor, viz. $\partial T/\partial t = -\mathbf{u}\cdot\nabla T$. This means that the cumulative temperature change will be greater when the velocity advects cooler water over an extended time period, assuming the temperature gradient remains about the same. Velocity is more persistent during the southward wind part of the stress ISO, and so that is when the temperature changes the most. In other words, the overall temperature change results from the time integral of velocity (or, equivalently, the time integral of the wind stress).

Ecosystem Simulations

A five-component, numerical ecosystem model (nitrate, ammonium, phytoplankton, zooplankton, and detritus) was coupled to a 3D circulation model and driven by the atmospheric forcing observed during COAST (7, 14). The applied wind stress was the 36-HLP filtered stress from NDBC 46050 (Fig. 3*a*), so it contained both the weather-band and intraseasonal components. The stress was applied in a spatially uniform fashion over the domain. Ecosystem variables display clear ISOs in response to the ISO component in the wind stress, with minimal weather-band variations. The ISO periodicities in modeled phytoplankton biomass and zooplankton biomass (Fig. 3 *b* and *d*), are in good agreement with those in observed chlorophyll-a and cope-

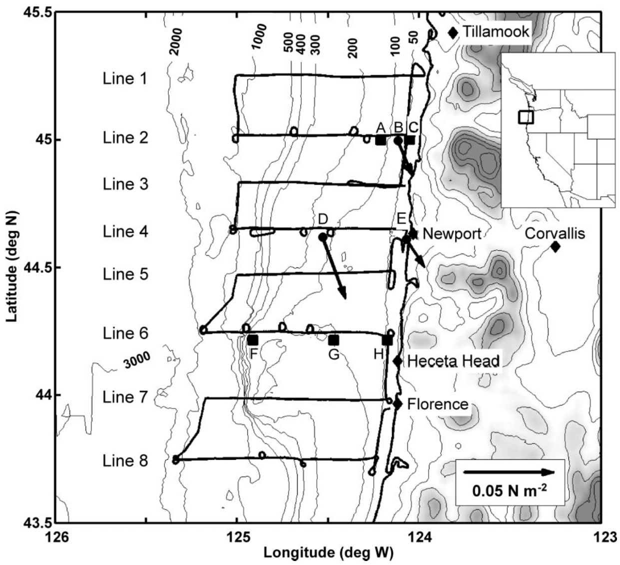

Fig. 4. Map of the COAST study area during summer 2001 (3). A typical survey track of eight east–west lines is shown (the black line in a ''radiator'' pattern). Three oceanographic instrument moorings were located on Line 2 [from west to east: NSB (A), NMS (colocated with the COAST MB) (B), and NIS (C)], and three were located on Line 6 [from west to east: SSB (F), SMS (G), and SIS (H)]. The three surface meteorological sites are shown as solid dots: the COAST MB on Line 2 (B), NDBC buoy 46050 on Line 4 (D), and the NWPO3 C-MAN station at Newport (E). The mean wind stress for May through August, 2001, at each met site is shown. Ocean bathymetric contours are in meters. The height contour interval over land is 500 m.

pod concentrations (Fig. 3 *c* and *d*). There is a time lag of several days between the maximum upwelling-favorable (downwelling-favorable) wind stress and the maximum (minimum) phytoplankton biomass (see Table 1), consistent with the time it takes the coastal upwelling circulation to bring nutrient-rich waters into the euphotic zone to fuel primary production. There is an additional several-day lag between fluctuations in phytoplankton concentration and those in zooplankton concentration due to the zooplankton feeding and growth times. The generation time for copepods to develop from an egg to an adult is temperature dependent, and for Oregon coastal waters it will range from ≈20 days at 15°C to 45 days at 10°C (15). The partition between new and regenerated production (*f*-ratio) shows similar ISO behavior with regenerated production being more important during the downwelling-favorable phase of the ISOs. The horizontal advection–diffusion balance also shows the alternation of offshore and onshore transport on the shelf with an intraseasonal periodicity, and this could potentially be important in retaining biomass on the shelf through reduction of the mean offshore transport.

Observed Phytoplankton and Zooplankton Variations

Data from an optical sensor moored near the 200-m isobath west of Newport were converted to phytoplankton biomass, and the results are shown in Fig. 3*c*. The 8-DLP filtered curve is shown; however, the original data follow this curve very well. There is scatter in the original unfiltered data about this curve, likely due to small-scale patchiness moving past the fixed-point sensor, but the measured biomass values are quite small at most times except during the five ISOs that can be seen clearly in the 8-DLP curve. There is reasonable qualitative agreement between this curve and the unfiltered model phytoplankton curve (Fig. 3*b*), except during the first ISO in May. It is not completely clear at this point why this difference occurs early in the time series, but it is likely that the model's initial condition set the phytoplankton concentration too high. It is also possible that the real-world phytoplankton concentrations were actually similar to the model values, but the spatial distribution was such that low phytoplankton concentrations happened to be located near the single-point moored sensor in May. Even so, for most of the time period the observed phytoplankton variability exhibited primarily ISOs that were generally in phase with, and about the same relative magnitude as, the modeled phytoplankton ISOs. The correlation between 8-DLP alongshore wind stress and observed phytoplankton is −0.58 (significant at the 95% level), with a lag of 13.6 days (Table 1).

Insolation is an additional factor affecting primary production. Although its relative importance is not known at this point, COAST observations show that insolation varied significantly on the 20-day time scale, with higher levels of short-wave radiation during southward winds: that is, when the North Pacific High dominated the region. These were also the times that the phytoplankton population increase rates were greatest.

Cruises have been made along the Newport Hydrographic Line (Line 4 in Fig. 4) at approximately biweekly intervals since 1996 to determine nutrient, chlorophyll, and zooplankton fields. The zooplankton observations made during the COAST time frame are shown in Fig. 3*d* along with the modeled zooplankton time series. Although the observed data points, due to the ≈2-week intervals between samples, will not by themselves resolve 20-day ISOs, their generally good correspondence with the model zooplankton time series in relative magnitude suggests that the real-world zooplankton total biomass varied along with the other oceanic variables on the 20-day time scale. This result is as expected, given the ISOs in observed phytoplankton biomass.

Discussion

A central feature of the Oregon coastal system is demonstrated in Figs. 2 and 3. Even though the coastal ocean is driven by a wind stress that has two energetic periodicities (2- to 6-day weather-band fluctuations and ISOs of ≈20-day periods), the significant response in many oceanic variables, including upper-ocean temperature, phytoplankton, and zooplankton, is on the ≈20-day time scale. The underlying reason why the phytoplankton and zooplankton biomasses are greatest on this time scale is relatively straightforward: This longer period of uninterrupted upwelling favorable winds, driven by the JS ISO activity, brings a continued supply of nutrients in upwelled water, and this provides for continued primary production. A greater total phytoplankton biomass results, and greater zooplankton biomass follows after the time required for growth. These growth episodes end when the JS ISO moves to the south and interrupts the upwelling winds.

Although the existence of upwelling events due to prolonged southward wind episodes has been apparent off Oregon for some time (17), what was not known until COAST was the cause for these episodes and the dominant effect they can have on setting the periodicity in the coastal ecosystem. We now see that when the JS is in a northward ISO phase, the North Pacific High builds into the region and drives the coastal winds southward, and they blow essentially uninterrupted until the JS moves back to the south. When in a southern ISO phase, the JS allows ETCs to pass over the region, and this decreases or reverses the upwelling favorable winds for a day to a few days during each ETC passage. This breaks the nutrient supply and decreases in primary and secondary production result.

Coastal upwelling occurs along most of the west coast of the United States and Mexico each summer, so it is of interest to know how JS ISOs affect other parts of this coastal region. Moving southward along the coast from Oregon, one gets farther from the JS, so it is anticipated that its ISO influence will diminish. The alongshelf extent of the JS's impact is not known, however. Off central California, intraseasonal variations in wind stress, water temperature, and sea level occur on the 40- to 60-day time scale (2), suggesting the source of these fluctuations is the tropical Madden–Julian ISO (18) and not JS ISOs. However, the analysis technique used was limited to periods from 30 to 70 days. We examined the wind-stress time series for 2001 from NDBC 46013 off Monterey, CA, and find the main ISO activity to be on the 35-day time scale [consistent with the findings in ref. 2] and on the 15-day time scale. These latter variations are likely JS driven, because it has been shown that there is a variance peak in the JS ISO activity in the northern hemisphere at $\approx$2 weeks (6). Wind-driven sea level variations with periods in the 40- to 60-day band have been found along the Pacific coast of North America (19, 20), again consistent with Madden–Julian forcing. However, these studies also did not consider fluctuations with periods of $<$30 days. The overall importance to the coastal ecosystem of the forcing on all of these intraseasonal scales remains to be established.

New Questions

This insight leads to a number of questions about the impact of JS-driven ISOs on this wind-driven coastal system and possibly on other midlatitude coastal regions. These questions include the following. Are there other oceanic forcing functions that vary with intraseasonal periodicities that could impact the coastal oceanic system, for example air–sea heat fluxes, oceanic stratification, and upper-ocean turbulent mixing? Will improved understanding of ISOs in atmospheric forcing increase predictive skill for the coastal ocean on the several-day, intraseasonal, and even superseasonal time scales? As global warming and climate changes occur, will the ISO activity in the atmosphere change in a manner that fundamentally alters ISO-forced coastal systems? Additionally, because it is known that a small fraction of the summers in this region do not experience ISOs in the alongshore wind stress, it is reasonable to ask: How will this ecosystem differ in years without ISOs as compared with years with ISOs? For example, will there be differences in ecosystem structure and/or overall biomass production when the nutrient delivery to the coastal system happens only on the 2- to 6-day time scale as opposed to on the 20-day time scale?

Materials and Methods

Near-surface water temperature was measured at all COAST mooring sites but NMS (see Fig. 4) with Sea-Bird Electronics sensors (SBE 39) at a depth of 2.4 m, except at MB where the sensor was located 1.5 m deep. At MB other meteorological variables were also measured, including incoming shortwave solar radiation (pyranometer LI200X; Li-Cor, Lincoln, NE) and wind velocity at 3-m height (R. M. Young, Traverse City, MI; product 05103-5). Data were collected at NDBC buoy 46050, located just south of Line 4, $\approx$35 km offshore of Newport on the 130-m isobath, and at the NDBC NWPO3 C-MAN station, located on the beach at Newport. Sensor heights/depths, relative to sea level for NDBC 46050 (NWPO3) were as follows: air temperature, 4.0 m (15.5 m); wind velocity, 5.0 m (18.5 m); ocean temperature, 0.6 m (N/A) (3). Wind stress was calculated by using measurements from NDBC buoy 46050 (3, 16).

The latitudinal position of the JS was taken as the location, along 125°W longitude (this passes through the COAST domain, just west of center; see Figs. 1 and 4), of the strongest horizontal gradient in the height of the 200-hPa surface (3), determined from 6 hourly National Centers for Environmental Prediction (NCEP) reanalysis pressure maps (21).

As part of the GLOBEC North East Pacific and COAST programs, a comprehensive *in situ* bio-optical and chemical dataset was obtained between 2000 and 2004 to characterize the spatial and temporal variability in the distribution of phytoplankton off the Oregon Coast (descriptions of cruise tracks and objectives may be found at http://damp.coas.oregonstate.edu/coast and http://globec.oce.orst.edu/groups/nep). This effort included the deployment of subsurface fluorometers and scatterometers on 4 GLOBEC moorings along the coast from May 2000 to April 2003, including one along the Newport Hydrographic line (Fig. 3*c*), the deployment of two spectroradiometers on COAST moorings during 2001 and 2003, and the analyses of discrete water samples collected during GLOBEC and COAST mesoscale cruises. Analyses included particulate absorption spectra, flow-cytometry, phytoplankton pigment composition by high-performance liquid chromatography (HPLC), and photosynthetic activity through fast repetition rate (FRR) or pulse-amplitude modulated (PAM) fluorometry.

Cruises have been made along the Newport Hydrographic Line at approximately biweekly intervals since 1996. Samples were taken at distances of 1, 3, 5, 10, 15, 20, and 25 nautical miles from shore (water depths range from 20 to 300 m). At each station the following was done: a CTD cast (SBE-19), a Secchi depth reading, a surface bucket sample for later analysis of nutrients and chlorophyll, and a vertical zooplankton net tow from just above the sea floor to the sea surface (or from a maximum depth of 100 m in deep water) by using a 0.5-m diameter, 200-μm mesh net. The number of cruises per year varied between 20 and 32. During the upwelling season (late April through September), cruises were often done more frequently than biweekly, ranging from 2.8 cruises per month (1998) to 3.8 cruises per month (2002). Copepods are the most abundant taxa in the samples, comprising 75–90% of the total biomass. Copepods from the zooplankton samples have been enumerated by species and developmental stage, and copepod biomass was calculated on dry weight and carbon content of species and stages. Each sample has been enumerated in detail, and stress ISOs can be compared with a number of zooplankton time series, including: changes in total biomass at a single station, individual species biomass at a given station, differences in community structure estimated from ordination and cluster analysis, differences in species diversity, and cross-shelf differences in biomass and/or species composition (22).

We thank S. Haines and E. Monbureau for data analysis and figure preparation, W. Waldorf and D. Root for building and deploying the COAST moorings, S. Gard for data archiving and analysis, and M. Levine and T. Boyd for providing moored velocity data. This work was supported by National Science Foundation Coastal Ocean Processes Program Grants OCE-9907854 and OCE-9907919.

1. Lau W, Waliser D (2005) *Intraseasonal Variability in the Atmosphere-Ocean Climate System* (Springer–Praxis, Chichester, UK).
2. Breaker L, Liu P, Torrence C (2001) *Cont Shelf Res* 21:727–750.
3. Bane J, Levine M, Samelson R, Haines S, Meaux M, Perlin N, Kosro P, Boyd T (2005) *J Geophys Res* 110:C10S02.
4. Barth JA, Menge BA, Lubchenco J, Chan F, Bane JM, Kirincich AR, McManus M, Nielsen K, Pierce S, Washburn L (2007) *Proc Natl Acad Sci USA* 104:3719–3724.
5. Lott F, Robertson A, Ghil M (2004) *J Atmos Sci* 61:1259–1283.
6. Ghil M, Kondrashov D, Lott F, Robertson A (2003) *Intraseasonal Oscillations in the Mid-Latitudes: Observations, Theory, and GCM Results*, preprint. Available at: www.atmos.ucla.edu/tcd/PREPRINTS/ECMWF.pdf.
7. Spitz Y, Allen J, Gan J (2005) *J Geophys Res* 110:C10S17.
8. Austin J, Barth J (2002) *J Geophys Res* 107:3180.
9. Bond N, Mass C, Overland J (1996) *Mon Wea Rev* 124:430–445.
10. Nuss W, Bane J, Thompson W, Holt T, Dorman C, Ralph F, Rotunno R, Klemp J, Skamarock W, Samelson R, *et al.* (1999) *Bull Am Meteorol Soc* 81:719–743.
11. Lentz S (1992) *J Phys Oceanogr* 22:1517–1539.
12. Kosro P (2005) *J Geophys Res* 110:C10S06.
13. Castelao R, Barth J (2005) *J Geophys Res* 110:C10S04.
14. Gan J, Allen J (2005) *J Geophys Res* 110:C10S07.
15. Peterson WT (2001) *Hydrobiologia* 453/454:91–105.
16. Large W, Pond S (1981) *J Phys Oceanogr* 11:324–336.
17. Smith RL (1974) *J Geophys Res* 79:435–443.
18. Madden RA, Julian PR (1994) *Mon Wea Rev* 122:814–837.
19. Spillane MC, Enfield DB, Allen JS (1987) *J Phys Oceanogr* 17:313–325.
20. Enfield DB (1987) *J Phys Oceanogr* 17:1860–1876.
21. Kistler R, Kalnay E, Collins W, Saha S, White G, Woollen J, Chelliah M, Ebisuzaki W, Kanamitsu M, Kousky V, *et al.* (2001) *Bull Am Meteorol Soc* 82:247–267.
22. Peterson W, Keister J (2003) *Deep-Sea Res* 50:2499–2517.